

**Photothermal deflection measurement on heat transport in GaAs epitaxial layers**

Sajan D George,\* P. Radhakrishnan, V. P. N. Nampoori, and C. P. G. Vallabhan

*International School of Photonics, Cochin University of Science and Technology, Cochin, India-682 022*

(Received 26 March 2003; revised manuscript received 27 May 2003; published 16 October 2003)

In this paper, we report the in-plane and cross-plane measurements of the thermal diffusivity of double epitaxial layers of *n*-type GaAs doped with various concentrations of Si and a *p*-type Be-doped GaAs layer grown on a GaAs substrate by the molecular beam epitaxial method, using the laser-induced nondestructive photothermal deflection technique. The thermal diffusivity value is evaluated from the slope of the graph of the phase of the photothermal deflection signal as a function of pump-probe offset. Analysis of the data shows that the cross-plane thermal diffusivity is less than that of the in-plane thermal diffusivity. It is also seen that the doping concentration has a great influence on the thermal diffusivity value. Measurement of *p*-type Be-doped samples shows that the nature of the dopant also influences the effective thermal diffusivity value. The results are interpreted in terms of a phonon-assisted heat transfer mechanism and the various scattering process involved in the propagation of phonons.

DOI: 10.1103/PhysRevB.68.165319

PACS number(s): 78.20.Nv, 66.30.Xj, 61.72.Vv, 66.70.+f

**INTRODUCTION**

The thermal characterization of layered structures has been a subject of great interest due to their wide applicability in the microelectronic and optoelectronic industry. A number of recent review articles highlighted the fact that the thermal conductivity and diffusivity of thin layers differ considerably from that of a corresponding bulk specimen due to the difference in microstructures such as the grain size, amorphous nature, and concentration of foreign atoms and defects, which strongly affects the scattering process of energy carriers.<sup>1</sup> In the case of layered structures, the interface thermal resistance and scattering of heat carriers at the boundary also contribute to a reduction in thermal conductivity and thermal diffusivity. Besides that, thin layers of a specimen with the same nominal composition as that of the bulk sample are reported to exhibit anisotropy and inhomogeneity. The effective thermal properties of layered structures are essentially determined by the properties of individual layers and the thickness of each layer. As the doping along with layer thickness can influence the thermal and transport properties of semiconductors in a substantial manner,<sup>2</sup> a detailed study of anisotropic heat transport and hence the thermal diffusivity value of layered structures has great physical and practical significance.

Since its discovery, the photothermal method has been used for the determination of several material properties of thin semiconducting layers, which are not easy to measure using conventional spectroscopic methods.<sup>3</sup> All photothermal methods are essentially based on the detection of thermal waves generated in the specimen after illumination with either pulsed or chopped optical radiation. Among the various photothermal methods used for investigating the material parameters, the laser-induced photothermal deflection (PTD) technique possesses some unique characteristics and advantages compared to other approaches.<sup>4</sup> The PTD technique is essentially based on the effect of a refractive index variation associated with a temperature gradient induced in the sample surface. In the past, this technique has been employed in different configurations viz., collinear PTD and transverse

PTD (mirage technique). These methods have been successfully employed to determine the optical absorption coefficient and thermal parameters of semiconductors and layered structures.<sup>5</sup> However, not much work has been done to probe the influence of the type of dopant and the doping concentration on thermal properties such as the thermal diffusivity of layered semiconductors.

In the present paper, we describe the in-plane and cross-plane measurements of the thermal diffusivity of GaAs multilayer samples. Thermal diffusivity is an important thermal transport property, reliable knowledge of which is of great interest in high-density electronics,<sup>6</sup> especially from the device fabrication point of view. Thermal diffusivity essentially determines the diffusion of heat and, physically, the inverse of thermal diffusivity is a measure of the time required to establish thermal equilibrium in a system in which a transient temperature change has occurred.<sup>7</sup> Among the various experimental configurations to evaluate the thermal diffusivity of solids using the PTD technique, the strategy used in the present investigation is the measurement of the PTD signal phase as a function of pump-probe offset at a fixed modulation frequency.<sup>8</sup> The phase data have been used here because, unlike the amplitude, the phase data do not depend on the heat beam intensity, but depend only on the periodic temperature at the sample surface.<sup>5</sup>

**THEORY**

A variety of detection configurations can be employed for the thermal and optical characterization of a material using the PTD technique.<sup>9</sup> Among these, the skimming PTD technique is simple and the most accepted approach for the thermal characterization of materials. The details of this configuration are explained elsewhere.<sup>10</sup> In the skimming PTD configuration, the specimen is irradiated with a chopped and focused laser radiation and the subsequent periodic nonradiative deexcitation of the specimen produces periodic thermal waves. Such periodic thermal waves create a corresponding refractive index variation in the coupling medium (usually a liquid with a high  $dn/dT$  value), which is in contact with the

specimen. A low-power probe beam skimming along the sample surface is used to monitor this refractive index gradient (RIG). The RIG is essentially based on the parameters of the specimen under investigation. Thus the probe beam on passing through a spatially varying RIG suffers deflection from its normal path. The amplitude as well as the phase of the PTD signal is dependent on the thermal and optical parameters of the specimen under investigation<sup>11</sup> and hence the measurement of signal enables the characterization of the sample properties.

For a Gaussian probe beam propagating through an inhomogeneous medium, most of the parameters can be deduced from the analysis made by Mandelis and Royce.<sup>12</sup> The propagation of a Gaussian beam through a spatially varying refractive index is given by the expression

$$\frac{d}{ds} \left( n_0 \frac{dr_0}{ds} \right) = \nabla_{\perp} n(r,t), \quad (1)$$

where  $r_0$  is the perpendicular displacement of the beam from its original direction.  $n_0$  is the uniform index of refraction and  $\nabla_{\perp} n(r,t)$  is the gradient of index of refraction perpendicular to the ray's path. Equation (1) can be integrated over the ray's path:

$$\frac{dr_0}{ds} = \frac{1}{n_0} \int_{path} \nabla_{\perp} n(r,t) ds, \quad (2)$$

where  $s$  is the optical path length. Because the deviation is small, one can get the deflection  $\Phi(t)$  as

$$\frac{dr_0}{ds} = \Phi(t) = \frac{1}{n_0} \frac{\partial n}{\partial T} \int_{path} \nabla_{\perp} T(r,t) ds, \quad (3)$$

where  $\nabla_{\perp} T(r,t)$  is the temperature gradient perpendicular to the ray's path. The deflection  $\Phi(t)$  can be resolved into two components  $\Phi_n$  and  $\Phi_t$ , which are, respectively, the deflections normal and parallel to the sample surface. Let the probe beam make a transverse offset  $y$  with respect to the pump beam axis and a vertical offset  $z$  with respect to the sample surface. The temperature field distribution, which is due to the pump beam absorption, obtained by the solution of heat diffusion equations in the sample as well as in the coupling fluid leads to the evaluation of  $\Phi_n$  and  $\Phi_t$  as

$$\begin{aligned} \Phi_n = & -\frac{1}{\pi n} \frac{dn}{dt} \int_0^{\infty} \cos(\delta y) A \\ & \times \exp(-\beta_0 z) \beta_0 d \delta \exp(j\omega t) \text{ for } z > 0 \end{aligned} \quad (4)$$

and

$$\begin{aligned} \Phi_t = & -\frac{1}{\pi n} \frac{dn}{dt} \int_0^{\infty} \sin(\delta y) A \\ & \times \exp(-\beta_0 z) \delta d \delta \exp(j\omega t) \text{ for } z > 0, \end{aligned} \quad (5)$$

where  $A$  is a complex integration constant,  $\delta$  is a spatial Fourier-transformed variable, and  $\beta_0 = (\delta^2 + j\omega/D_0)^{1/2}$ , where  $D_0$  is the thermal diffusivity of the coupling fluid.

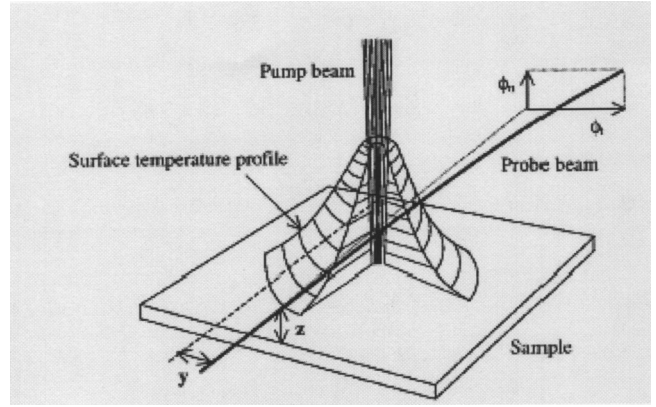


FIG. 1. Schematic diagram of the probe beam skimming PTD configuration;  $y$  and  $z$  are the transverse and vertical offsets, respectively.

A linear relationship between the PTD signal phase as well as the amplitude with various parameters such as pump-probe offset (the lateral distance between the pump and probe beam) and height of the probe beam above the sample surface has already been reported.<sup>11</sup> For  $a = b = z = 0$ , where  $a$ ,  $b$ , and  $z$  are the pump beam spot size, probe beam spot size, and probe beam height above the sample surface, there is a linear relation between the phase of the PTD signal and the pump-probe offset. This linear relation is found to be applicable in three different configurations of pump and probe: (1) Probe beam skimming configuration with pump and probe on the same side of the sample, (2) probe beam skimming configuration with pump and probe on different sides of the sample, and (3) probe beam passing through the sample. The first configuration is used in the present investigation. In this configuration, the slope of the plot connecting the phase of the PTD signal and pump-probe offset is given by

$$m = \frac{1}{\mu_s} = \left( \frac{\pi f}{\alpha_s} \right)^{1/2}. \quad (6)$$

Here the suffix  $s$  indicates the sample and  $f$  denotes the chopping frequency of incident radiation. In practice, the condition  $a = b = z = 0$  cannot be achieved. However, for the specimens with moderately high thermal diffusivity value, Eq. (6) holds good for finite values of  $a$ ,  $b$ , and  $z$  (Refs. 6 and 11). Recent studies show that, by considering the interface as a charge-trapping region, both two-layer and mono-layer approximations yield identical responses for modulated photothermal studies.<sup>13</sup> The evaluation of the anisotropic thermal diffusivity of Al/Ti multilayers has already been reported.<sup>14</sup> A schematic of the probe skimming configuration is given in Fig. 1.

## EXPERIMENT

$n$ -type and  $p$ -type GaAs thin films grown upon semi-insulating GaAs substrates were used as samples in the in

TABLE I. Details and thermal diffusivity value of the samples under investigation. 1, 2, 3, and 4 represent the sample numbers.

Sample	$l$ ( $\mu\text{m}$ ) <sup>a</sup>	$n$ ( $\text{cm}^{-3}$ ) <sup>b</sup>	Thermal diffusivity value ( $\text{cm}^2 \text{s}^{-1}$ )	
			In plane	Cross plane
<sup>1</sup> Si-doped GaAs (upper)	0.20	$2.0 \times 10^{18}$	$0.142 \pm 0.0006$	$0.113 \pm 0.0004$
<sup>1</sup> Si-doped GaAs (middle)	1.80	$2.0 \times 10^{18}$		
<sup>1</sup> Semi-insulating GaAs (substrate)	400.00			
<sup>2</sup> Si-doped GaAs (upper)	0.20	$2.0 \times 10^{16}$	$0.155 \pm 0.0004$	$0.122 \pm 0.0005$
<sup>2</sup> Si-doped GaAs (middle)	2.80	$2.0 \times 10^{16}$		
<sup>2</sup> Semi-insulating GaAs (substrate)	400.00			
<sup>3</sup> Si-doped GaAs (upper)	0.25	$3.6 \times 10^{14}$	$0.172 \pm 0.0004$	$0.135 \pm 0.0005$
<sup>3</sup> Si-doped GaAs (middle)	10.00	$3.6 \times 10^{14}$		
<sup>3</sup> Semi-insulating GaAs (substrate)	400.00			
<sup>4</sup> Be-doped GaAs (upper)	0.20	$2.0 \times 10^{18}$	$0.130 \pm 0.0003$	$0.105 \pm 0.0004$
<sup>4</sup> Be-doped GaAs (middle)	1.80	$2.0 \times 10^{18}$		
<sup>4</sup> Semi-insulating GaAs (substrate)	400.00			

<sup>a</sup>Thickness of the layer.

<sup>b</sup>Concentration of dopant.

vestigation. The thin films were grown by the molecular beam epitaxial method (Applied Physics Department, Technical University of Eindhoven, Eindhoven, The Netherlands). All the samples contained two epitaxial layers. The sample structure together with the specifications of each layer and the dopant concentration is given in Table I. For convenience we have labeled the samples arbitrarily as 1, 2, 3, and 4.

Continuous optical radiation at 488 nm from an argon ion laser (Liconix 5300), which is mechanically chopped (Stanford Research Systems SR 540), is used as the source of excitation. The laser beam has a Gaussian profile with a diameter of 1.2 mm. In all the measurements the power is kept at 50 mW ( $\pm 0.5\%$ ) and the incident radiation is chopped at 10 Hz so that  $\omega\tau \ll 1$ . Hence only the thermal diffusion process contributes to the heat transport of the samples under investigation. The excitation photon energy, viz., 2.54 eV, is much greater than the band gap energy of GaAs (1.43 eV) and the entire incident radiation is absorbed at the surface ( $\sim 1 \mu\text{m}$ ) of the epitaxial layer itself. Consequently, all the specimens are considered to be opaque at the incident wavelength. Moreover, the fact that the entire energy is absorbed at the surface of the sample implies that heat is generated on the surface of the epitaxial layer and it propagates through the entire structure. The pump beam is focused using a convex lens having a focal length of 20 cm so as to get a spot size of  $100 \mu\text{m}$  on the sample surface. Carbon tetrachloride ( $\text{CCl}_4$ ) is used as the coupling liquid for the present investigation due to its high thermal diffusivity value ( $\alpha = 7.31 \times 10^{-4} \text{ cm}^2 \text{ s}^{-1}$ ) and very high rate of change of refractive index with temperature ( $dn/dT = 6.12 \times 10^{-4} \text{ K}^{-1}$ ) (Ref. 15). A 4-mW He-Ne laser (Uniphase) emitting at 633 nm is used as a probe beam to detect the strength of the refractive-

index gradient in  $\text{CCl}_4$ . The probe beam also has a Gaussian profile with a beam diameter of  $700 \mu\text{m}$  and it is focused with a convex lens having a focal length of 8 cm to a spot size of  $90 \mu\text{m}$  at the point of pump-probe crossing. The probe laser beam is arranged such that it just skims through the sample surface, and it propagates along the  $y$  direction, which is orthogonal to the pump beam ( $z$  axis). A position-sensitive quadrant detector is used to measure the deflection of the probe beam. The output of the quadrant detector is fed to a dual phase lock-in amplifier (Stanford Research Systems SR 830). The entire experimental setup is laid out on a vibration-isolated table top to protect the system from ambient vibrations. A schematic view of the experimental setup is shown in Fig. 2. In the present configuration, the distance

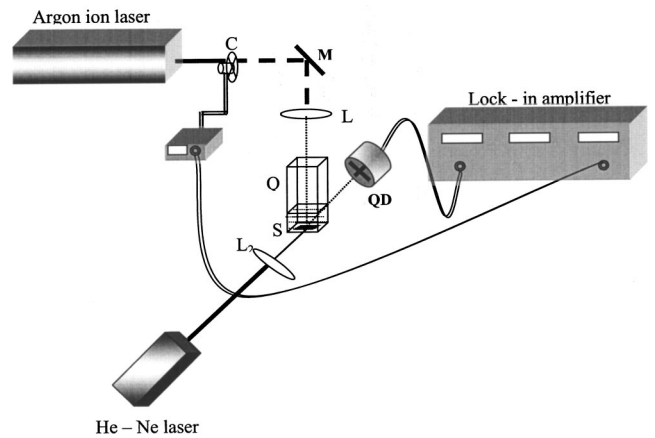


FIG. 2. Schematic view of the experimental setup: M, mirror;  $L_1$ ,  $L_2$ , lenses; C, chopper; Q, cuvette; S, sample; QD, quadrant detector.

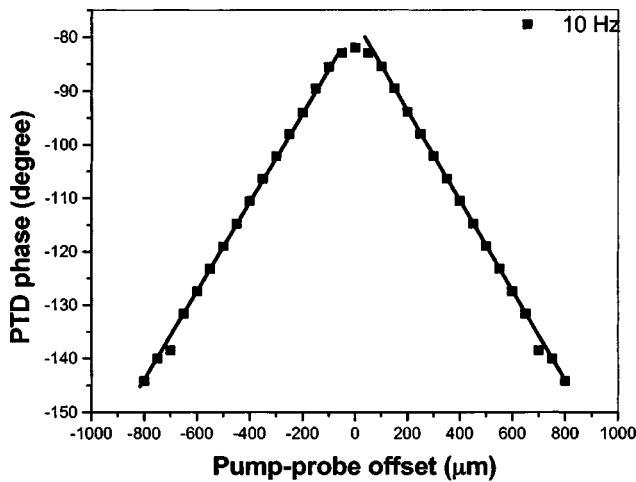


FIG. 3. Variation of PTD signal phase with pump-probe offset for sample 1 in the normal direction.

between the probe and sample surface is kept as small as possible so as to get a nondiffracted beam (from the sample edge) at the detector head.

**RESULTS AND DISCUSSION**

Figure 3 shows the variation of the PTD phase in the normal direction as a function of pump-probe offset for sample 1 whereas Fig. 4 shows the variation of the PTD phase in the transverse direction as a function of pump-probe offset. Thermal diffusivity is evaluated from the slope of the plot on either side of the point of excitation and the average value of the two measurements is also given in Table I. It has been found that the thermal diffusivity is to be less than the earlier reported value of bulk GaAs.<sup>3</sup> All other samples also show similar behavior (not shown). The thermal diffusivity values measured along the in-plane and cross-plane directions for all specimens under investigation are depicted in Table I. From the table it is seen that the thermal diffusivity of the samples varies with the concentration of dopant and it

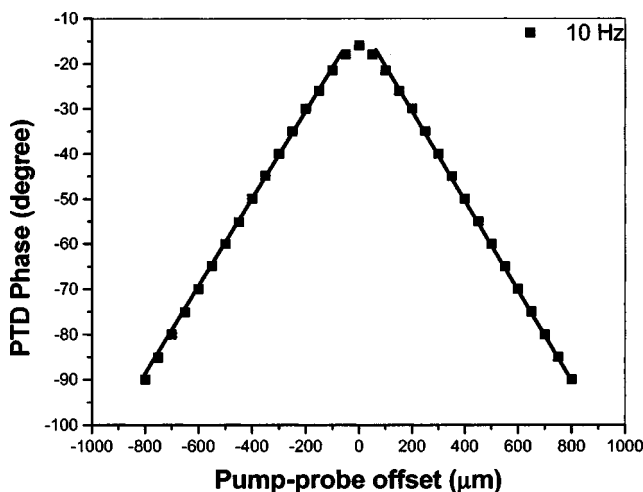


FIG. 4. Variation of PTD signal phase with pump-probe offset for sample 1 in the transverse direction.

is even sensitive to the nature of the dopant. In the case of semiconductors, thermal energy is essentially carried away by electrons and holes.<sup>16</sup> However, in the case of semiconductors with low or normal density of carriers, at all temperatures well below their melting point, the heat conduction process is primarily due to phonons.<sup>17</sup> Thermal conductivity and hence thermal diffusivity are determined by the phonon mean free path, which in turn depends on the phonon velocity and its relaxation time.<sup>18</sup> The propagation of phonons through the lattice suffers various scattering mechanisms such as phonon-phonon scattering, phonon-electron scattering, and scattering of phonons by the crystal boundaries and defects. In the case of semiconductors, at room temperature, the scattering of phonons is caused by the anharmonicity in the interatomic potential energy function.<sup>19</sup> The electron-phonon scattering obviously depends on the carrier concentration and is important only at very high carrier concentration. In the present investigation, substrates of all the specimens are semi-insulating in nature so that the contribution from the carriers is negligibly small. However, phonon scattering from crystal imperfections, point defects, and impurities can be major contributing factors in determining the effective thermal conductivity (thermal diffusivity) value. In the case of semiconductors, it is the propagation of acoustic phonons that is more effective in determining the thermal parameters as compared to optical phonons.<sup>19</sup>

The detected photothermal signal from a semiconductor is not solely dependent upon how heat is carried away by each quasiparticle system in the semiconductor and its thermal parameters (electron and phonon thermal diffusivity and thermal conductivity) but also on how energy and momentum are distributed between them; i.e., the detected signal depends greatly on various scattering mechanisms suffered by the heat carriers.<sup>16</sup> However, in the case of layered semiconductors the reduction in their effective thermal parameters<sup>20</sup> depends mainly on (a) the doping effect, (b) the interface effect, and (c) the quantum size effect. In the present investigation, the epitaxial layers have thicknesses much greater than the mean free path of phonons in GaAs (~10–20 Å) so that quantum confinement has a negligible influence in our investigations. Hence the phonon spectrum in each layer can be represented by its bulk form.<sup>19</sup> Since the epitaxial layer thickness is greater than the phonon mean free path, the normal and umklapp scattering rates are identical to those for the bulk specimen.<sup>21</sup> The normal scattering processes are significant for longitudinal and low-frequency transverse phonons, whereas umklapp scattering is the dominating phenomenon for high-frequency transverse phonons. At room temperature, the high-frequency transverse phonons are the effective carriers of heat.<sup>22</sup> In addition to these scattering mechanisms, phonons also suffer scattering from impurities present in the epitaxially grown layers, which in turn reduces the phonon mean free path and, hence, the phonon group velocity. The reduction in phonon mean free path or phonon group velocity results in the reduction of the lattice thermal conductivity ( $k = Cv\Lambda/3$ , where  $C$  is the volumetric specific heat,  $v$  is the phonon group velocity, and  $\Lambda$  is the phonon mean free path) and hence the effective thermal diffusivity value. It has already been reported that the lattice

thermal conductivity  $k$  is governed by the lattice thermal resistivity ( $W$ ) through the relation  $k = 1/W = BT^{-n}$  (where  $n$  is a constant at a particular temperature and  $B$  is a parameter which decreases with increase in doping concentration) and it decreases with an increase in doping concentration.<sup>23</sup> It is interesting to point out here that the thermal diffusivity value of the  $p$ -type specimen is small as compared to the  $n$ -type specimen. This is due to the fact that the scattering rate of phonons due to impurities is proportional to the square of the mass difference between gallium and the dopant atom. In Be:GaAs, beryllium is much lighter than silicon; the mass difference between silicon and gallium is less in comparison to the mass difference between the beryllium and gallium. Thus the phonons in the Be-doped  $p$ -type specimen suffer a large scattering rate and thus result in a reduced value for thermal diffusivity for the sample.

The interface effects also play a significant role in the reduction of thermal diffusivity of layered structures as compared to bulk specimen. As the thickness of epitaxial layers is relatively larger than the phonon mean free path, interface scattering cannot be either completely diffusive or specular in nature.<sup>24</sup> Specular interface scattering depends on the mismatch in acoustic impedance and phonon group velocity between the two layers. If the roughness of the interface is comparable to the wavelength of the phonon, diffuse scattering at the interface will dominate in the interface scattering mechanism. In the present case the layers are doped with impurities and they are grown by the molecular beam epitaxial method so that interface scattering is both diffusive and specular in nature.<sup>24</sup> A small increase in diffuse scattering due to an increase in dangling bonds at the interface caused by the variation in doping levels can affect the thermal diffusivity value in a substantial manner.<sup>19</sup> When the interface roughness is of the order of the phonon mean free path, it can act as an effective diffusive interface scattering center for phonons which results in the reduction of thermal diffusivity value.<sup>19</sup> The inelastic scattering caused by the anharmonic interatomic force due to doping and the phonon mode conversion at the interface can also result in the diffuse scattering mechanism. This thermal barrier resistance (TBR) due to interface roughness results in the reduction of the thermal diffusivity value. However, the effect of interface roughness is relatively small as compared to the doping effects. In addition to these scattering mechanisms, dislocations in the epitaxially grown layers result in internal scattering, which in turn causes a reduction in thermal diffusivity. In order to predict the exact contribution from each factor to the reduction in the thermal diffusivity value, a more detailed investigation and theoretical modeling based on the propagation of various longitudinal and transverse acoustic phonons and its reflection and transmission at the interface is needed. Nevertheless, the present investigation shows that the effective thermal diffusivity values in the in-plane and cross-plane measurements show a considerable decrease as compared to the bulk specimen.<sup>25</sup>

It is seen from the measurements that the thermal diffusivity values of the specimens under investigation follow a logarithmic dependence with doping concentration. It was reported<sup>26</sup> earlier that the phonon scattering rate is given by

the expression  $A\omega^4$ , where  $\omega$  is the phonon angular frequency.  $A$  is a constant related to the doping concentration and is given by

$$A = \frac{nV^2}{4\pi v_s^3} \left( \frac{\Delta M}{M} \right)^2,$$

where  $n$  is the dopant concentration,  $V$  is the volume of the host atom,  $v_s$  is the average phonon group velocity,  $M$  is the atomic mass of the host atom, and  $\Delta M$  is the difference between the host and impurity atoms. The above relation suggests a linear decrease in the thermal diffusivity value with doping concentration. However, the experimentally observed logarithmic dependence could be due to the combined effect of both doping concentration and the thickness of the epitaxial layers.<sup>26</sup> An increase in the thermal conductivity value of layers with specimens having thickness of the order of the  $\mu\text{m}$  range has already been reported.<sup>18</sup> It can be attributed to the increase in spectral phonon heat capacity as well as to the reduction in total relaxation time with size.<sup>27</sup> As mentioned earlier, at 300 K only the high-frequency transverse phonons are the effective carriers of heat. The net effect of the increase in phonon heat capacity is the reduction of the amount of heat carried away by each phonon. The typical relaxation time of the umklapp process at 300 K is about  $10^{-9}$  s, corresponding to a relaxation length of the order of a micron. This indicates that even in the specimens having thickness of the order of  $\mu\text{m}$  (Ref. 27), as in the present investigation, the size of the epitaxial layer has an effect on the effective thermal diffusivity value.

The cross-plane thermal diffusivity is less as compared to the in-plane thermal diffusivity value. The phonons parallel to the film have a greater phonon mean free path as compared to those in the perpendicular direction, resulting in a larger thermal diffusivity value in the parallel direction.<sup>22</sup> In general, the measured thermal resistance of the film in the cross plane consists of two parts: viz., thermal resistance within the film and the thermal boundary resistance at the interface.<sup>20</sup> The interface and boundary scattering have larger effect on the mean free path of phonons propagating perpendicular to the point of excitation.<sup>19,20</sup> This is due to the temperature jump experienced by the phonons at the interface.<sup>20</sup> However, in the in-plane direction local thermal equilibrium is established in a length scale much smaller than the length of the specimen in that direction. The anisotropy in the thermal properties of freestanding thin films has already been reported.<sup>22</sup> As the interface contains a large number of dangling bonds it acts as effective scattering centers for phonons, which in turn results in a reduced value for thermal diffusivity along the perpendicular direction as compared to the parallel direction. Thus the physical anisotropy of the epitaxial layers results in the anisotropy of the measured effective thermal diffusivity value of all samples under investigation.

## CONCLUSION

In conclusion, measurements of anisotropic thermal diffusivity on GaAs double epitaxial layers have been carried out.

It is seen that the layered structures show a substantial reduction in the effective thermal diffusivity value as compared to those reported earlier in a bulk specimen. The in-plane thermal diffusivity is found to be larger as compared to its cross-plane value. Analysis of the results shows that the nature of the dopant as well as the doping concentration has a pronounced effect on the propagation of thermal waves and hence on the thermal diffusivity value. The present study also suggests that in the case of layered structures, the mean free path of phonons in the tangential direction is relatively large in comparison to the mean free path in the perpendicular direction. This can be ascribed to additional scattering of phonons in the normal direction due to the interface and thermal boundary resistance of the epitaxial layers.

## ACKNOWLEDGMENTS

The authors wish to acknowledge Professor J. H. Wolter and Dr. J. E. M. Haverkort (COBRA Group, Technical University of Eindhoven, The Netherlands) for their constant encouragement as well as for providing the semiconductor samples used in this report. S.D.G. acknowledges the Council of Scientific and Industrial Research, New Delhi for providing financial assistance. He also wishes to acknowledge useful discussion with Dr. A. Deepthy and Dilna. S. during the preparation of this manuscript. V.P.N.N. also acknowledges University Grant Commission, New Delhi for financial assistance through a research award project. This work is supported by Netherlands University Federation For International Collaboration (NUFFIC), The Netherlands under MHO assistance to the International School of Photonics.

\*Electronic address: sajan@cusat.ac.in

- <sup>1</sup>Albert Feldman and Naira M. Valzeretti, *J. Res. Natl. Inst. Stand. Technol.* **130**, 107 (1998); D. G. Chill, *J. Vac. Sci. Technol. A* **7**, 1259 (1990); L. Hatta, *Int. J. Thermophys.* **11**, 293 (1990); K. E. Goodson and M. I. Flik, *Appl. Mech. Rev.* **47**, 101 (1994); C. L. Tien and G. Chen, *J. Heat Transfer* **116**, 799 (1994).
- <sup>2</sup>I. Riech, P. Diaz, and E. Marin, *Phys. Status Solidi B* **220**, 305 (2000); G. Chen and M. Naegu, *Appl. Phys. Lett.* **71**, 2761 (1997).
- <sup>3</sup>*Photoacoustic and Thermal Wave Phenomena in Semiconductors*, edited by A. Mandelis (Elsevier, New York, 1987); H. Vargas and L. C. M. Miranda, *Phys. Rep.* **161**, 43 (1988); *Photothermal Investigations of Solids and Fluids*, edited by J. A. Sell (Academic, New York, 1988); A. Pinto Neto, H. Vargas, N. F. Leite, and L. C. M. Miranda, *Phys. Rev. B* **41**, 9971 (1990).
- <sup>4</sup>A. Rosecwaig, *Photoacoustic and Photoacoustic Spectroscopy* (Wiley Interscience, New York, 1983); *Photoacoustic and Photothermal Phenomena*, edited by P. Hess and J. Pelzl (Springer-Verlag, Berlin, 1988).
- <sup>5</sup>S. Faycel, *Opt. Mater. (Amsterdam, Neth.)* **12**, 163 (1999); W. A. McGahan and K. D. Kole, *J. Appl. Phys.* **72**, 1362 (1992); D. Fournier, V. Bocara, A. Skumanich, and N. M. Amer, *ibid.* **59**, 787 (1986).
- <sup>6</sup>M. Bertolotti, R. L. Voti, G. Liakhov, and C. Sibila, *Rev. Sci. Instrum.* **64**, 1576 (1993); A. Salzar, A. S. Lavega, and J. Fernandez, *J. Appl. Phys.* **69**, 1216 (1991); P. K. Wong, P. C. W. Fung, and H. L. Tam, *ibid.* **84**, 6623 (1998).
- <sup>7</sup>M. Soltanolkotabi, G. L. Bennis, and R. Gupta, *J. Appl. Phys.* **85**, 794 (1999); Sajan D. George, S. Dilna, P. Radhkrishnan, C. P. G. Vallabhan, and V. P. N. Nampoori, *Phys. Status Solidi A* **195**, 416 (2003).
- <sup>8</sup>*Photoacoustic and Photothermal Phenomena III*, edited by D. Bicanic (Springer-Verlag, Berlin, 1992).
- <sup>9</sup>W. B. Jackson, N. M. Amer, C. Boccara, and D. Fournier, *Appl. Opt.* **20**, 1333 (1981); M. Bertolotti, G. Liakhov, R. Li Voti, A. Matera, C. Sibila, and M. Valentino, *Opt. Eng. (Bellingham)* **36**, 515 (1997).
- <sup>10</sup>Nibu A. George, C. P. G. Vallabhan, V. P. N. Nampoori, and P. Radhkrishnan, *Appl. Opt.* **41**, 5179 (2002).
- <sup>11</sup>A. Salzar and A. S. Lavega, *Rev. Sci. Instrum.* **65**, 2896 (1994).
- <sup>12</sup>A. Mandelis and B. S. H. Royce, *Appl. Opt.* **23**, 2892 (1984).
- <sup>13</sup>C. Christofides, F. Diakonov, A. Seas, C. Christou, M. Nestoros, and A. Mandelis, *J. Appl. Phys.* **80**, 1713 (1996).
- <sup>14</sup>E. J. Gonzalez, J. E. Bonevich, G. R. Stafford, G. White, and D. Josell, *J. Mater. Res.* **15**, 764 (2000).
- <sup>15</sup>S. E. Bialkoswski, *Photothermal Spectroscopy Method Chemical Analysis* (Wiley, New York, 1996).
- <sup>16</sup>A. F. Carballo Sanchez, G. Gonzalez de la Cruz, Yu. G. Gurevich, and G. N. Logvinov, *Phys. Rev. B* **59**, 10 630 (1999).
- <sup>17</sup>B. Yang and G. Chen, *Phys. Low-Dimens. Semicond. Struct.* **5/6**, 37 (2000).
- <sup>18</sup>Yu. G. Gurevich, G. Gonzalez de la Cruz, G. N. Logvinov, and N. M. Kasyanchuck, *Semiconductors* **32**, 1179 (1998).
- <sup>19</sup>G. Chen, *Phys. Rev. B* **57**, 14 958 (1998); *Trans. ASME* **119**, 220 (1997).
- <sup>20</sup>S. Y. Ren and J. D. Dow, *Phys. Rev. B* **25**, 3750 (1982); T. Zeng and G. Chen, *J. Heat Transfer* **132**, 340 (2001).
- <sup>21</sup>M. G. Holland, *Phys. Rev.* **132**, 2461 (1963).
- <sup>22</sup>C. Chen, C. L. Tien, X. Wu, and J. S. Smith, *J. Heat Transfer* **116**, 325 (1994).
- <sup>23</sup>Sadao Adachi, *Physical Properties of III-V Semiconductor Compounds* (Wiley, New York, 1992).
- <sup>24</sup>X. Wang, H. Hu, and X. Xu, *Trans. ASME* **123**, 138 (2001).
- <sup>25</sup>A. Calderon *et al.*, *J. Appl. Phys.* **84**, 6327 (1998).
- <sup>26</sup>Angela D. McConnell, Srinivasan Uma, and K. E. Goodson, *J. Microelectromech. Syst.* **10**, 360 (2001).
- <sup>27</sup>G. Chen and C. L. Tien, *J. Thermophys. Heat Transfer* **7**, 311 (1993).